NJC

Accepted Manuscript

This is an *Accepted Manuscript*, which has been through the Royal Society of Chemistry peer review process and has been accepted for publication.

Accepted Manuscripts are published online shortly after acceptance, before technical editing, formatting and proof reading. Using this free service, authors can make their results available to the community, in citable form, before we publish the edited article. We will replace this *Accepted Manuscript* with the edited and formatted *Advance Article* as soon as it is available.

You can find more information about *Accepted Manuscripts* in the Information for Authors.

Please note that technical editing may introduce minor changes to the text and/or graphics, which may alter content. The journal's standard Terms & Conditions and the Ethical guidelines still apply. In no event shall the Royal Society of Chemistry be held responsible for any errors or omissions in this *Accepted Manuscript* or any consequences arising from the use of any information it contains.

ROYAL SOCIETY OF CHEMISTRY

www.rsc.org/njc

Photoluminescent and Cytotoxic Properties of Multinuclear Complexes and Multinuclear-based Polymers with Group 12 Metals and Tripodal Ligand

Jin'an Zhao,*[a] Kun Peng,[b] Yan Guo,[b] Jin Zhang,[b] Shufang Chen,[a] and Jiyong Hu*[a]

Four novel multinuclear complexes and multinuclear-based polymers with group 12 metal centers, namely, $Zn_3(tpbb)Cl_6$ (**1**), $\{[Cd_6(tpbb)_2Cl_{12}]\cdot 2CHCl_3\cdot 0.5H_2O\}_n$ (**2**), $Hg_4(tpbb)Br_8$ (**3**), and $Hg_4(tpbb)I_8$ (**4**), have been synthesized with respect to a new flexible tripodal ligand, 1,3,5-Tris((2-(pyridine-2-yl)-1H-benzo[d]imidazol-1-yl) methyl) benzene (tpbb). Complex **1** is a trinuclear cluster, after being determined by X-ray crystallography, while **2** features an unprecedented hexanuclear metallacycle-based 2D network with chloride ion bridges. The similar umbrella-like tetranuclear architecture of **3** and **4** with different Hg(II)-halide salts demonstrate that halide with the same tetrahedral coordination geometry of metal center do not greatly affect the structure of the complexes. Photoluminescent studies indicate that complexes **1** and **2** reveal enhanced and red-shifted solid-state fluorescence at room temperature compared with ligand tpbb, while **3** and **4** show prominent phosphorescence behaviors at cryogenic temperatures with lifetimes in microsecond range. Additionally, being tested against a panel of several human carcinoma cell lines (SH-SY5Y, QBC939 and EC109) by standard MTT assay, complex **1** displayed potential cytotoxicity against SH-SY5Y and QBC939 cells, and selectivity to different tumor cell lines.

Introduction

Generation of multinuclear complexes is of great prosperity as a consequence of their diverse fascinating functionalities for potential applications in areas like pharmaceutical, photoluminescent and magneto-chemistry.[1] Meanwhile, as interest in the field of metallosupramolecular chemistry continues to grow, fabrication of multinuclear-based polymers, which possess more stable and intriguing high-dimensional architectures and topologies, is also pretty significant. In recent years, Sun *et.al* conducted in-depth research to construct multinuclear complexes and multinuclear-based polymers, and several high-nuclear silver clusters as well as multinuclear silver-based polymers with interesting structures were reported.[2] Being an important class of multinuclear complexes and multinuclear-based polymers, compounds containing group 12 elements are particularly attractive for many reasons: the variety of coordination numbers and geometries provided by the d^{10} configuration of the group 12 metal ions, photoelectric properties, fluorescence properties, widespread applications of group 12 compounds, the essential role in biological systems of zinc, and so on.[3] Thus, the design of different multinuclear complexes and multinuclear-based polymers with group 12 metal centers becomes a pivotal task, in which the organic ligands play a very crucial role.

Tripodal ligands, because of the disparity of physicochemical and structural features displayed by their metal complexes,[4] have received considerable attention. From the previously reported studies, N-heterocyclic tripodal ligands have been proved to be one of the most useful organic connectors for the construction of novel multinuclear complexes and multinuclear-based polymers with specific structures and interesting properties. For example, Sun and co-workers have constructed a series of cage-like complexes through the application of 1,3,5-tris(imidazol-1-ylmethyl)-2,4,6-trimethylbenzene.[5] Recently, in the group of Zheng, four polymers with specific structures and topologies were reported by assembly of Cd(II) and Co(II) with an N-centered tripodal ligand.[6] Among the reported N-heterocyclic tripodal ligands, most contained pyridyl or imidazolyl groups as donors, the ones tethered with benzimidazole unit, however, are relatively rare. Wang group have reported some Cu(I) and Pt(II) trinuclear structures by utilizing a rigid benzimidazole-containing tripodal ligand, 1,3,5-tris[2-(2-pyridyl)benzimidazolyl]benzene, as the connector.[7] In contrast to the rigid tripodal ligands with little or no conformational changes when they interact with metal salts, the flexible tripodal ligands have much more possible coordination modes than the rigid ones due to their flexibility and low symmetry, since the flexible ligands can adopt different conformations according to the geometric needs of different metal ions.[8]

Taking the aforementioned perspectives into consideration, an unexplored tripodal ligand, 1,3,5-Tris((2-(pyridine-2-yl)-1H-benzo[d]imidazol-1-yl) methyl) benzene (tpbb), in which the coordinating benzimidazole groups were connected to pyridyl units as well as to the central aromatic ring through the methylene, was synthesized in our group (Scheme 1). A variety of multinuclear complexes and multinuclear-based polymers could be expected for such flexible ligand not only has the merit of benzimidazole, which allow easy derivation and potentially strong $\pi\cdots\pi$ stacking interaction to form supramolecular structures, but also bears the virtue of $-CH_2-$ that can freely bend and rotate to interact with metal centers.[9] Herein, four group 12 metal-based complexes with tpbb, namely, $Zn_3(tpbb)Cl_6$ (**1**), $\{[Cd_6(tpbb)_2Cl_{12}]\cdot 2CHCl_3\cdot 0.5H_2O\}_n$ (**2**), $Hg_4(tpbb)Br_8$ (**3**), and

[a] *College of Chemical and Material Engineering, Henan University of Urban Construction, Pingdingshan, Henan 467036, P.R. China Fax: 86-375-2089090, E-mail: zjinan@zzu.edu.cn*
[b] *College of Chemistry and Molecular Engineering, Zhengzhou University, Zhengzhou, Henan, 450052, P.R. China*
† Electronic Supplementary Information (ESI) available: crystallographic data for the structural analysis have been deposited with the Cambridge Crystallographic Data Center, CCDC reference numbers 1038024-1038027. These data can be obtained free of charge via www.ccdc.cam.ac.uk/conts/retrieving.htm (or from the Cambridge Crystallographic Data Centre, 12, Union Road, Cambridge CB2 1EZ, UK; fax: +44 1223 336033).

New Journal of Chemistry Accepted Manuscript

$Hg_4(tpbb)I_8$ (**4**), were generated. Photoluminescent studies indicate that complexes **1** and **2** exhibit enhanced and red-shifted solid-state fluorescence at room temperature compared with ligand tpbb, while **3** and **4** demonstrate prominent phosphorescence behaviors at cryogenic temperatures with lifetimes in microsecond range. Additionally, being tested against a panel of several human carcinoma cell lines (SH-SY5Y, QBC939 and EC109) by standard MTT assay, complex **1** displayed potential cytotoxicity against SH-SY5Y and QBC939 cells and selectivity to different tumor cell lines.

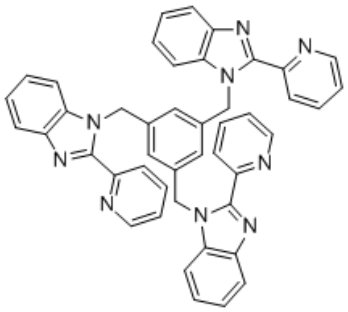

Scheme 1. The structure of tpbb.

Results and Discussion

Crystal structure of $Zn_3(tpbb)Cl_6$ (1).

The molecular structure of complex **1** crystallizes in a trigonal system, space group R-3, yet with the three Zn(II) centers chelated by tpbb, which has a *cis, cis, cis*-conformation in **1** and acts as a tridentate linker using its three arms to coordinate with three Zn atoms in the same manner as depicted in Fig. 1 (for structure as thermal ellipsoid model, see Fig. S1). In each fragment, one Zn(II) ion assumes a distorted tetrahedral geometry via coordinating with two nitrogen atoms (N1, N3) from benzimidazole and pyridyl groups as well as two Cl^- (Cl1, Cl2) with the average Zn–N and Zn–Cl bond distances are 2.060 and 2.204 Å, respectively. The bond angles around Zn(II) ions vary from 78.95(12)° to 119.61(11)°.

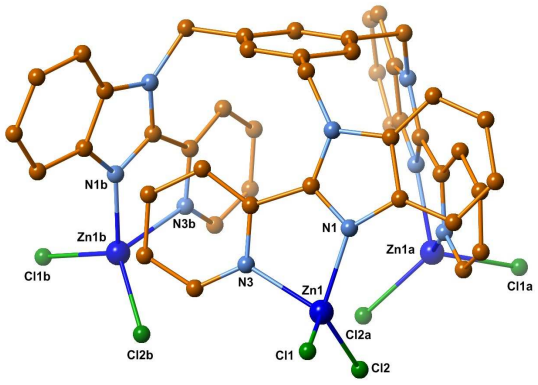

Fig. 1 The trinuclear framework of complex **1** (all hydrogen atoms and solvent molecules are omitted for clarity).

The structure of **1** is stabilized by face-to-face π···π interactions between the adjacent imidazole ring and pyridine ring with centroid separation of 3.832(4) Å and the dihedral angle of 11.2(3)° (1-x, 1-y, 1-z). Further, the trinuclear motif is, which can be seen in Fig. S2, stabilized by C13–H13A···$Cl1^A$ hydrogen bond (3.620(5) Å) (^{A}4/3-y, 2/3+x-y, -1/3+z),[10] and the structures are ultimately connected into a 3D supramolecular network by the hydrogen-bonding as well as the π···π interactions.

Crystal structure of $\{[Cd_6(tpbb)_2Cl_{12}]\cdot 2CHCl_3\cdot 0.5H_2O\}_n$ (2).

Complex **2** belongs to the trigonal system with R-3 space group. As seen in Fig. 2a (for structure as thermal ellipsoid model, see Fig. S3), the octahedral Cd atom is six-coordinated by two N atoms from one tpbb with the bond lengths of Cd1–N1, Cd1–N2 being 2.443(10) and 2.339(8) Å, and the four remaining sites of Cd are occupied by four chloride anions with the bond lengths of Cd1–Cl1, Cd1–Cl1', Cd1–Cl2, and Cd1–Cl2' being 2.678(3), 2.642(2), 2.546(3), and 2.590(3) Å, respectively. In complex **2**, chloride anions from decomposed solvent of chloroform serve as the bridge to two neighboring Cd(II) ions, and the Cd–Cd distance in **2** is 3.824(16) Å, much longer than that observed in the metal (2.980 Å).[11] The bond angle of Cl2'–Cd1–Cl1 is 84.08(8)°, close to a right angle. Interestingly, as shown in Fig. 2b, with the same coordination manner, six Cd atoms comprise an unprecedented hexanuclear metallacycle through the bridging of chloride atoms. For the tripodal ligand, each tpbb adopts a *propeller*-conformation and binds with three Cd atoms and extended complex **2** into a 2D network (Fig. 2c).

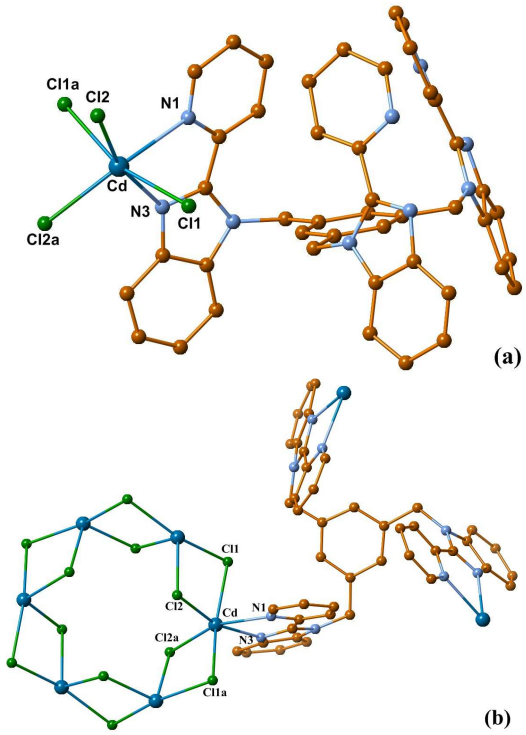

New Journal of Chemistry Accepted Manuscript

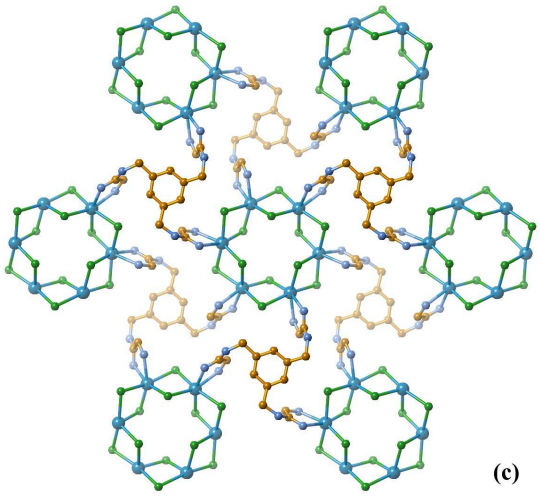

Fig. 2 (a) The coordination environment of metal center in complex **2** (all hydrogen atoms and solvent molecules are omitted for clarity). (b) The hexanuclear metallacycle comprised by Cd centers and chloride anions. (c) The 2D network of complex **2** (all hydrogen atoms and solvent molecules are omitted for clarity).

Ultimately, the 2D network is further connected into a 3D supramolecular framework (Fig. S4) by the π···π interactions between imidazole ring and pyridine ring (3.820 (8) Å) (5/3-x, 4/3-y, 4/3-z) as well as hydrogen bonding interactions (3.685(14) Å for C10–H10···Cl1^{A}, 3.587(15) Å for C13–H13B···Cl1^{B}, and 2.846(19) Å for C15–H15···N10^{C}) (^{A}4/3-y, 2/3+x-y, -1/3+z; ^{B}5/3-x, 4/3-y, 4/3-z; ^{C}2-y, 1+x-y, z).

Crystal structure of $Hg_4(tpbb)Br_8$ (3) and $Hg_4(tpbb)I_8$ (4).

Ligand tpbb was reacted with $HgBr_2$ and HgI_2, respectively, to see the effect of the halide on the structure of the complexes. Similar cell parameters and the results of crystallographic analyses confirm that **3** and **4** are isostructural, and there is no great influence of Br^- and I^- on the structure of them. Thus, as an example, only the structure of complex **3** is described here in detail.

Single crystal X-ray crystallographic analysis reveals that complex **3** crystallizes in a trigonal system, space group R-3, yet with a tetranuclear motif. As presented in Fig. 3 (for structure as thermal ellipsoid model, see Fig. S5), the structure of **3** comprises neutral $Hg_3Br_6(tpbb)$ moieties and $HgBr_2$ molecules to result a thirteen-component umbrella-like framework: four metal centres, one tpbb ligand and eight bromine atoms. In the umbrella bones, the tripodal ligand, tpbb, with *cis, cis, cis*-conformation and serves as a tridentate linker to coordinate with three Hg(II) atoms by the same coordination mode to form an equilateral triangle with an edge length (Hg1–Hg1A separation) of 7.447 Å. The Hg1 atom is coordinated by two bromine anions (Br1, Br2) and two nitrogen atoms (N1, N2) from a benzimidazole group and one pyridyl unit of tpbb, yielding a distorted tetrahedron. Bond lenghths for Hg1–Br1, Hg1–Br2, Hg1–N1 and Hg1–N2 are 2.529(2), 2.465(2), 2.437(16) and 2.246(14) Å, respectively. The two nitrogen atoms of the ligand tpbb chelate to the metal centre with a N1–Hg1–N2 bite angle of 69.3(5)°, which are similar with those of N–Hg–N in the literature.[12] As for the umbrella handle, the Hg2 atom is 2-fold coordinated by two terminal bromine anions in a linear arrangement (Br3–Hg2–Br4 180.0°), with bond length of 2.409 (4) and 2.419(4) Å for Hg2–Br3 and Hg2–Br4, which are comparable with those in the $HgBr_2$ molecules.[13] Additionally, taking the van der Waals radii of Hg and Br to be 1.70 and 1.95 Å,[14] any Hg···Br contact less than 3.65 Å may therefore potentially be considered significant, while the distance between Hg2 and Br2 in this complex is 3.229 Å, which can be defined as a weak contact. The similar structure of **4** is shown in Fig. S6 and Fig. S7.

In complex **3**, there exists π···π interactions between imidazole ring and pyridine ring (3.749 (8) Å) (1-x, 1-y, 1-z). Upon the basis of π···π interactions and the hydrogen bond (3.750(11) Å for C13–H13A···Br1^{A}) (^{A}2/3-y, 1/3+x-y, 1/3+z), the tetranuclear structures are finally extended into a 3D supramolecular architecture (Fig. S8).

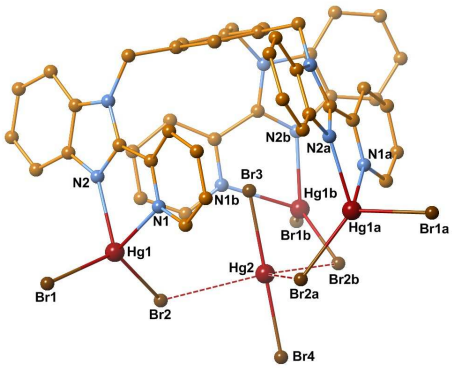

Fig. 3 The tetranuclear framework of complex **3** (all hydrogen atoms are omitted for clarity).

Effect of tpbb and anions on the Structures of Complexes 1–4.

The flexible ligand tpbb acted as a tris-bidentate connector and adopted different conformations to form complexes with varied structures. According to the position of three arms relative to the central benzene ring plane, two conformations of tpbb were defined, namely the *cis, cis, cis*-one: three arms are all located in the same side of the central benzene ring plane (Scheme 2a); the *propeller*-one: all the three arms are coplanar with and close to the benzene ring plane (Scheme 2b). The different conformations of tpbb, which are attributed to the flexible nature of the free $–CH_2–$ spacers, could greatly enrich the structures of complexes **1**–**4**. In complex **1**, tpbb acts as the *cis, cis, cis*-conformation to symmetrically link three $ZnCl_2$ groups and make it show trinuclear clusters. While in the case of **2**, tpbb applies the *propeller*-conformation, and the three arms of each tpbb are coordinated with Cd atoms from different hexanuclear metallacycle rings, which extended complex **2** into a 2D network. As for the isostructural complexes **3** and **4**, tpbb serves as the *cis, cis, cis*-conformation, and three HgX_2 (X=Br^- or I^-) groups occupy each of the three N,N-binding sites, and one of the two halide ligands further connects to a Hg center from the

New Journal of Chemistry Accepted Manuscript

linear HgX_2 unit, finally resulting in the tetranuclear umbrella-like architectures.

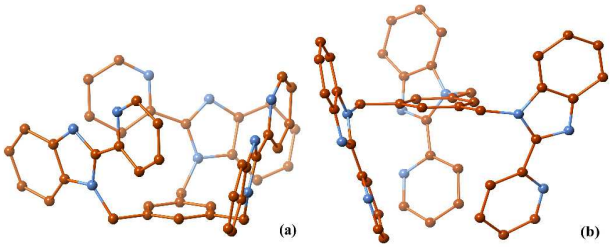

Scheme 2. (a) The *cis, cis, cis*-conformation of tpbb. (b) The *propeller*-conformation of tpbb.

The same umbrella-like tetranuclear architecture of **3** and **4** demonstrate that halides with the same tetrahedral coordination geometry of metal center do not greatly affect the structure of these Hg(II) complexes.

Thermogravimetric analysis of 1 and 2

Complex **1** and **2** are air-stable and can retain crystal integrity at ambient temperature. Thermogravimetric analysis (TGA) of **1** and **2** were carried out by heating to 1000°C. For complex **1**, the TGA curve (Fig. S9a) shows an initial weight loss of 3.16% taken place between 30°C and 290°C, which could be assigned to uncoordinated acetonitrile (Calcd 3.57%). The DSC spectrum exhibits an endothermic peak near 220°C, which also implies the loss of uncoordinated solvent. The endothermic peak near 326°C may indicate the melt of **1**. As for complex **2**, TGA curve (Fig. S10a) exhibits that the first weight loss of 8.07% taken place until 280°C, corresponding to two uncoordinated chloroform and half uncoordinated water (Calcd 9.02%). The endothermic peak around 250°C of DSC spectrum also suggests the loss of uncoordinated solvent. To further prove the existence of the solvent molecules in complexes **1** and **2**, their TGA spectra were also measured after heating to 100°C in vacuum for 10 h. The TGA spectra after treatment (Fig. S9b and Fig. S10b) display no initial weight loss for both of them before 300°C, demonstrating the existence of solvent molecules in the original complexes **1** and **2**.

Photoluminescent Properties.

Metal-organic coordination compounds, especially those with d^{10} metal centers, have been reported to be able to affect the emission wavelength and intensity of the organic material through metal coordination.[15] The luminescent behaviors of free ligand tpbb and complexes **1**–**4** were studied at room temperature in the solid state. The emission spectrum of tpbb features a strong band at 406 nm with an excitation band at 346 nm (Fig. S11). The emission spectra of complexes **1**–**2** (Fig. 4) closely resemble that of the free ligand with enhanced intensities and red shifts, and no clear luminescence was detected for complexes **3** and **4** under the same experimental condition. It can be observed that a broad emission with a maximum wavelength of 412 nm upon excitation at 378 nm for **1**. Complex **2** has a strong emission band centered at 440 nm with an excitation band at 369 nm, which is red-shifted by 34 nm compared with that of tpbb. The solid emission phenomena displayed by complexes **1** and **2** at room temperature are similar with those of other Zn(II) and Cd(II) complexes from literatures.[16] Since the Zn^{2+} and Cd^{2+} ions are difficult to oxidize or to reduce for their d^{10} configuration, the emissions of these complexes are neither the metal-to-ligand charge transfer (MLCT) nor the ligand-to-metal charge transfer (LMCT).[17] The observed emissions of complexes **1** and **2** are probably contributed by the π-π* intraligand fluorescence due to the similar emissions for ligand itself,[18] and the red shift of the emission maximum between the complexes and tpbb was considered to mainly originate from the influence of the coordination of metal atom to the ligand.

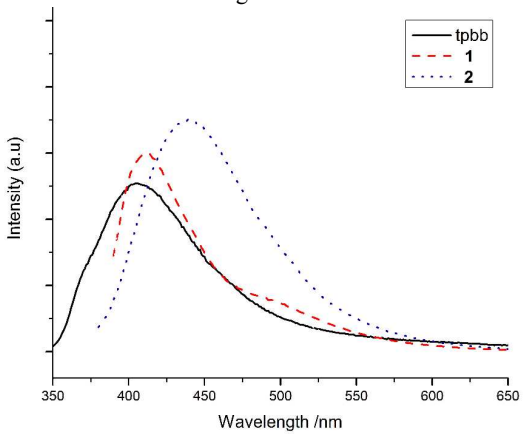

Fig. 4 The photoluminescence emission spectra of complex **1**, **2** and tpbb in the solid state at room temperature.

Though the luminescence for complexes **3** and **4** was quenched under the experimental condition, the two Hg(II) complexes are expected to show photoluminescence at cryogenic temperatures since as heavy atom, Hg(II) can effectively enhance the rate of intersystem crossing from singlet state to the triplet excited state and spin-orbit coupling effects,[19] which propelling us into investigating the photoluminescence properties of complexes **3** and **4** as well as tpbb in the solid state at a series of cryogenic temperatures. With the temperature cooling, the emission intensity of tpbb was enhanced, accompanying the negiligible bathochromic shift (Fig. S11). At 13K, 77K, 100K ,150K, 200K, 250K and 298K, lifetimes for solid tpbb yield τ = 4.169±0.039 ns, 4.069±0.036 ns, 3.841±0.037 ns, 3.522±0.035 ns, 3.291±0.032 ns, 3.021±0.029 ns, and 2.663±0.029 ns, respectively, indicating single-state emissions. The emission spectra of **3** (Fig. 5a), when excited at 290 nm, expressed two types of photoluminescence emission bands: fluorescence emission band at 398 nm with lifetimes in nanosecond order (0.111±0.013 ns at 298 K), and strong phosphorescence band at 528 nm with lifetimes in microsecond range, yield τ = 6.977±0.099 ms (13K), 5.541±0.139 ms (77K), 4.598±0.125 ms (100K), 3.611±0.042 ms (150K), 2.024±0.018 ms (200K), 1.186±0.022 ms (250K), and 0.606±0.033 ms (298K). Whereas complex **4** showed a weak fluorescence emission at 435 nm with nanosecond range lifetimes (0.162±0.005 ns at 298 K) as well as an intense phosphorescent emission maximum at λem = 526 nm (λex = 292 nm), respectively (Fig. 5b). The lifetimes of phosphorescence

New Journal of Chemistry Accepted Manuscript

band for **4** at cryogenic temperatures, yield τ = 3.021±0.053 ms (13K), 2.676±0.151 ms (77K), 1.734±0.013 ms (100K), 0.349±0.075 ms (150K), 0.461±0.040 ms (200K), 0.344±0.052 ms (250K), and 0.325±0.036 ms (298K), insinuating triplet-state emissions. The photoluminescence spectra of complexes **3** and **4** at different temperatures are consistent with the previously reported heavy metal-based complexes.[20] At room temperature, the large nonradiative rate constant makes it difficult to observe phosphorescence and, with temperature cooling, the phosphorescence intensity and lifetimes for **3** and **4** are gradually increased, which may be related to the inhibition of the nonradiative decay of the emitting triplet-excited state with decreasing temperature.[21] The subtle differences between lifetimes of **3** and **4** suggest that anions may have influence on the photoluminescence properties of complexes.

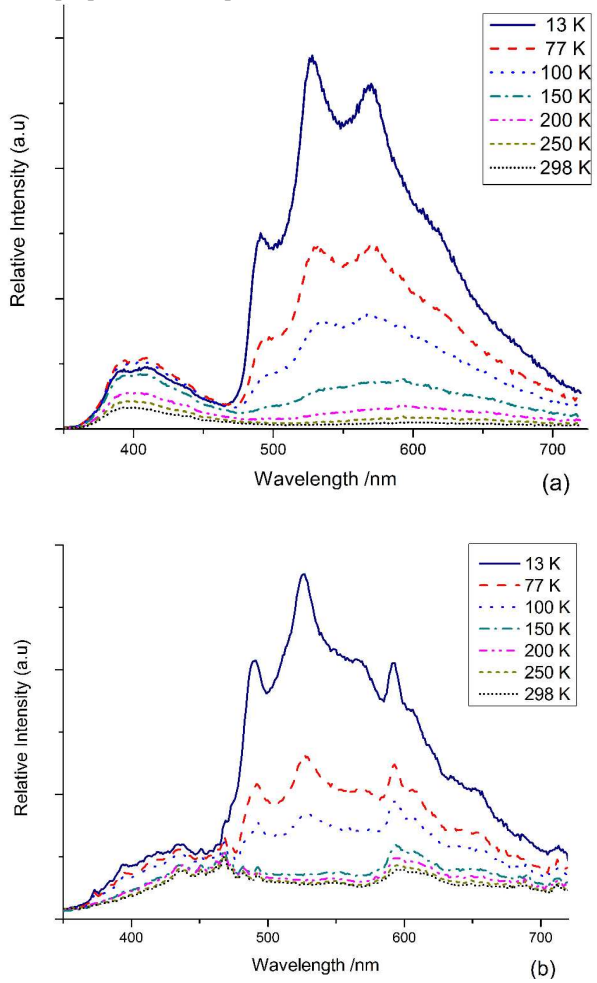

Fig. 5 (a) The photoluminescence emission spectra of complex **3** (λex = 290 nm) in the solid state at 298 K and low temperatures. (b) The photoluminescence emission spectra of complex **4** (λex = 362 nm) in the solid state at 298 K and low temperatures.

Cytotoxicity Results.

Since zinc plays the essential role in biological systems, the trinuclear Zn-based complex in this paper, **1**, was regarded as a potential candidate for fighting with cancer. Complex **1** was assessed with the standard MTT assays using for its cytotoxicity against a panel of three human carcinoma cell lines containing examples of SH-SY5Y (neuroblast tumor cell line), QBC939 (cholangio tumor cell line), and EC109 (esophagus tumor cell line) after different time. Complex **1** was dissolved in 5‰ DMSO and a blank sample with the same volume of DMSO was provided as a control at the same time. The concentrations of the complex ranged from 10 μM to 50 μM. The cytotoxicity of the complex was found to be concentration-dependent, which is to say that the average cell viability ratio decreased with increasing concentrations of the tested compounds. IC_{50} values, which can be seen in Fig. 6, were calculated from the dose-survival curves obtained after 24 h, 48 h and 72 h drug treatment from standard MTT test.

Among the selected tumor cell lines, complex **1** exhibited fast-acting, broad spectrum and the most effective on SH-SY5Y with IC_{50} values being 27.90 μM (24 h), 22.81 μM (48 h), and 17.84 μM (72 h). While when working against QBC939, complex **1** demonstrated not so strong cytotoxicity with IC_{50} values in 35–40 μM order. The cytotoxic effects of complex **1** against EC109 were considerably time-dependent. After 24 h, IC_{50} values were 65.15 μM, and the values decreased to 57.94 μM for 48 h then got to 51.06 μM another 24 h later. The distinguishing cytotoxic behaviors that complex **1** expressed on the three tumor cell lines elucidate that complex **1** has the selectivity towards different carcinoma cells.

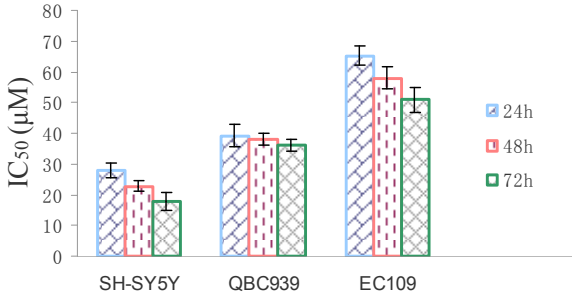

Fig. 6 The IC_{50} values of complex **1** against tumor cell lines.

To deeply understand its cytotoxic property, IC_{50} values of tpbb and cisplatin for 48 h were also investigated under the same experimental condition, and results are listed in Table 1. It was observed that the cells treated with tpbb were growth arrested but viable, and the IC_{50} values are generally three to six times compared with those of complex **1**, which could tentatively coincide with the synergic effect of combination of complex **1**. In comparison with the IC_{50} values of cisplatin, complexes with IC_{50} values less than 30 μM were considered to be strongly cytotoxic; complexes with IC_{50} values in the range of 30–50 μM were moderately cytotoxic; complexes with IC_{50} values in the range of 50–100 μM were regarded as being weakly antineoplastic; complexes with IC_{50} values over 100 μM were thought to be inactive.[22] Thus in terms of IC_{50} values, complex **1** has the potential to act as an effective metallopeptide-based chemotherapeutic agent targeting SH-SY5Y cells, while it is moderately cytotoxic against QBC939 and weakly antineoplastic towards EC109. In parallel with these findings, the cytotoxicities exhib-

New Journal of Chemistry Accepted Manuscript

ited by complex **1**, which are comparable with those of some promising Zn(II) complexes,[23] indicate that the present zinc complex demonstrates potent antitumor activity. Our work is in progress to comprehensively elucidate the mechanistic pathways employed by complex **1** against these tumor cell lines.

	IC_{50} values (μM)		
	SH-SY5Y	QBC939	EC109
1	22.8 ± 1.6	38.0 ± 2.0	57.9 ± 3.7
tpbb	132.9 ± 9.1	136.1 ± 4.6	169.8 ± 6.1
cisplatin	25.7 ± 2.1	126.9 ± 5.1	13.3 ± 0.3

Table 1. Comparison of the cytotoxic effects of complex **1**, tpbb and cisplatin (**(**IC_{50} values were tested for 48 h).

Stability of Complex 1 in Solution.

The stability of the complex in solution is important for biological studies. Complex **1** is soluble at 3×10^{-5} M concentration level in phosphate-buffered saline (PBS, 0.01 M, PH 7.4 at 25°C) containing 5‰ dimethylsulfoxide (DMSO). The kinetic UV-vis spectrum of complex **1** is shown in Fig. 7. Over the time course, the characteristic absorption of the complex displayed hypochromicity but no bathochromic shift. The hypochromicity can be attributed to the gradual formation of aggregates of the complex in solution, which will decrease its effective concentration for UV-vis absorption.[24] In a 72 h period, no significant changes were observed in the room temperature UV-vis spectrum, and no demetalation was observed in any case.[25] Additionally, the ESI-MS of complex **1** in DMSO (Fig. S12) showed peak at *m/z* 1142.3 is assigned to the formation of $[Zn_3(tpbb)Cl_7]^-$, which suggests that complex **1** remained the trinuclear structure in the solution. As for the other peaks at *m/z* 170.3, 306.1 and 443.9 are due to the fragmentation of the complex.[26] Since no significant changes in the UV-vis spectrum over the time course and peak of trinuclear structure was observed in the ESI-MS spectrum, we could deduce that complex **1** is stable in the solution.

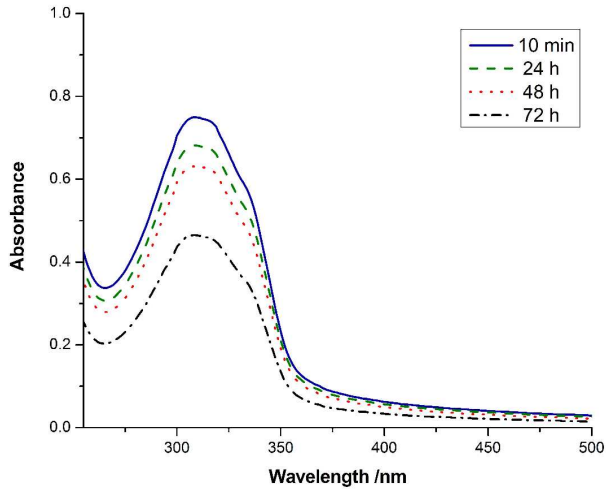

Fig. 7 Time-dependent stability studies on complex **1** in solution monitored by UV-vis absorption spectra.

Conclusions

Four novel multinuclear complexes and multinuclear-based polymers with group 12 metal centers, which feature various structures, were constructed with an unexploited flexible tripodal ligand and investigated their crystal structures and properties. Photoluminescent studies indicate that complexes **1** and **2** exhibited enhanced and red-shifted solid-state fluorescence at room temperature compared with ligand tpbb, while **3** and **4** demonstrated prominent phosphorescence behaviors at cryogenic temperatures with lifetimes in microsecond range. IC_{50} values for complex **1** alludes that it showed potential *in vitro* cytotoxicity against SH-SY5Y and QBC939 cells, and selectivity to different tumor cell lines.

Experimental Section

Materials and general methods.

All chemicals were obtained from commercial sources and used without further purification. The 1,3,5-Tris((2-(pyridine-2-yl)-1H-benzo[d]imidazol-1-yl) methyl) benzene (tpbb) was synthesized according to the reported procedures in the literature.[27] Cisplatin was purchased from Shanghai Energy Chemical Co., Ltd. IR spectra were recorded in the region of 400–4000 cm^{-1} with KBr pellets on a BRUKER TENSOR 27 spectrophotometer. Elemental analyses for C, H and N were carried out with a Flash EA 1112 elemental analyzer. Photoluminescence measurements for tpbb and complexes **1**–**4** at ambient temperature were carried out on Hitachi F–4600 Spectrofluorimeter, and photoluminescent properties of tpbb and complexes **3** and **4** were measured on Edinburgh Analytical Instruments FLS920 Spectrofluorimeter at cryogenic temperatures in solid state. UV-vis absorption spectra were performed on a Specord 200 UV-visible spectrophotometer. The ESI-MS spectra in DMSO were carried out on an Agilent 1100 LC/MSD Trap SL Electrospray Ionization Mass Spectrometer. The absorbance for MTT assay was measured at test wavelength of 492 nm using a Tecan Infinite M1000 Pro microplate reader. Thermogravimetric experiments were performed using a NETZSCH STA 449F3 instrument.

Syntheses.

$Zn_3(tpbb)Cl_6$ (1). A mixture of $ZnCl_2$ (0.0061 g, 0.03 mmol), tpbb (0.0070 g, 0.01 mmol), ethanol (1 mL), and acetonitrile (1 mL) was placed in a glass reactor (10 mL) which was heated at 85°C for 2 days and then gradually cooled to room temperature at a rate of 5°C/h. Yellow block crystals of **1** were obtained. Yield: 70% (based on Zn). Elemental Anal. Calcd for $Zn_3C_{45}H_{33}N_9Cl_6$ (%): C, 48.75%; H, 3.00%; N, 11.37%; Found (%): C, 47.99%; H, 3.25%; N, 11.63%. Element analysis was measured after heating complex **1** to 100°C in vacuum for 10 h. IR (KBr/pellet, cm^{-1}): 3443.68(s), 1573.08(w), 1485.17(m), 1431.63(s), 1346.28(w), 1015.21(w), 930.30(w), 818.92(w), 742.11(m), 621.35(w).

New Journal of Chemistry Accepted Manuscript

$\{[Cd_6(tpbb)_2Cl_{12}]\cdot 2CHCl_3\cdot 0.5H_2O\}_n$ (2). A mixture of $Cd(ClO_4)_2$ (0.0169 g, 0.04 mmol), tpbb (0.0070 g, 0.01 mmol), ethanol (9 mL) and chloroform (3 mL) was placed in a Teflon-lined stainless steel vessel (20 mL). The mixture was sealed and heated at 135°C and kept for three days, and then the reaction system was gradually cooled to room temperature at a rate of 5°C/h. Dark yellow crystals were obtained. Yield: 60% (based on Cd). Elemental Anal. Calcd for $Cd_6C_{92}H_{68}N_{18}Cl_{18}O_{0.5}$ (%): C, 40.24%; H, 2.50%; N, 9.18%; Found (%): C, 40.51%; H, 2.26%; N, 9.01%. IR (KBr/pellet, cm^{-1}): 3438.96(s), 1594.39(m), 1479.65(m), 1415.19(m), 1334.63(w), 1108.92(w), 991.73(w), 749.21(m), 622.63(w).

$Hg_4(tpbb)Br_8$ (3). A mixture of $HgBr_2$ (0.0144 g, 0.04 mmol), tpbb (0.0070 g, 0.01 mmol), methanol (1 mL), and acetonitrile (1 mL) was placed in a glass reactor (10 mL) which was heated at 80°C for 3 days and then gradually cooled to room temperature at a rate of 5°C/h. Yellow block crystals of **3** were obtained. Yield: 65% (based on Hg). Elemental Anal. Calcd for $Hg_4C_{45}H_{33}N_9Br_8$ (%): C, 25.24%; H, 1.55%; N, 5.89%; Found (%): C, 25.22%; H, 1.56%; N, 5.91%. IR (KBr/pellet, cm^{-1}): 3444.89(s), 1591.40(m), 1480.30(m), 1413.68(m), 1335.53(w), 1167.46(w), 1004.30(w), 817.70(w), 743.10(m), 632.06(w).

$Hg_4(tpbb)I_8$ (4). The synthesis of **4** was similar to that of **3**, except that HgI_2 (0.0182 g, 0.04 mmol) was used instead of $HgBr_2$. Yellow block crystals were obtained. Yield: 65% (based on Hg). Elemental Anal. Calcd for $Hg_4C_{45}H_{33}N_9I_8$ (%): C, 21.47%; H, 1.32%; N, 5.01%; Found (%): C, 21.50%; H, 1.36%; N, 4.96%. IR (KBr/pellet, cm^{-1}): 3454.50(s), 1569.27(m), 1477.62(m), 1413.66(m), 1334.67(w), 1121.79(w), 978.51(w), 816.43(w), 741.54(m), 622.93(w).

Crystal structure determination.

The single crystals suitable for X-ray determination were selected and mounted on a glass fiber separately. Data for complexes **1**–**4** were recorded on a SuperNova with graphite monochromated Cu-*K*α (λ = 1.54184 Å) for **1** at 293K and for **2** at 160K, and Mo-Kα radiation (λ = 0.71073 Å) for **3** and **4** at 293K. The structures were handled by direct methods and expanded with Fourier techniques. The calculations of complexes **1**–**4** were conducted with the Olex2 and SHELXL-97 crystallographic program.[28] Since the thermal vibration of solvent molecules in complex **1** are extremely large, the SQUEEZE subroutine of the PLATON software was used to subtract their contribution to the overall intensity data.[29] All the non-hydrogen atoms were refined with anisotropic thermal parameters. The final cycle of full-matrix least-squares refinement was based on the observed reflections and variable parameters. Table 2 and 3 give the crystallographic crystal data and structure processing parameters of the four complexes. The selected bond lengths and bond angles of them are listed in Table 4.

Cell culture.

SH-SY5Y, QBC939 and EC109 cells were routinely maintained in the logarithmic phase at 37°C in a highly humidified atmosphere of 95% air with 5% carbon dioxide, using DMEM medium for SH-SY5Y, and RPMI1640 medium for QBC939 and EC109. All mediums are supplemented with 10% (v/v) heat inactive fetal bovine serum (FBS).

Table 2. Crystal data and structure refinements for complexes **1** and **2**.

Complex	1	2
Empirical formula	$Zn_3C_{45}H_{33}N_9Cl_6$	$Cd_6C_{92}H_{68}N_{18}Cl_{18}O_{0.5}$
Formula weight	1108.61	2746.14
Temperature (K)	293(2)	160(10)
Wavelength (Å)	1.54184	1.54184
Crystal system	trigonal	trigonal
Space group	R-3	R-3
a (Å)	18.1422(4)	16.1561(8)
b (Å)	18.1422(4)	16.1561(8)
c (Å)	25.8426(5)	31.8535(14)
α (°)	90.00	90.00
β (°)	90.00	90.00
Γ (°)	120.00	120.00
Volume ($Å^3$), Z	7366.2(3), 6	7200.5(8), 3
F (000)	3348.0	4032.0
θ range for data collection(°)	3.29 to 76.52	3.45 to 76.58
Goodness-of-fit on F^2	1.072	1.006
Final R1[a], wR2[b]	0.0516, 0.1505	0.0766, 0.1986

[a]$R_1 = [|F_0| - |F_c|]/|F_0|$; [b]$wR_2 = [w(F_0^2 - F_c^2)^2]/[w(F_0^2)^2]^{1/2}$; $w = 1/[\sigma^2(F_o)^2 + 0.0297\ P^2 + 27.5680\ P]$, where $P = (F^2_o + 2\ F^2_c)/3$.

Table 3. Crystal data and structure refinements for complexes **3** and **4**.

Complex	3	4
Empirical formula	$Hg_4C_{45}H_{33}N_9Br_8$	$Hg_4C_{45}H_{33}N_9I_8$
Formula weight	2141.44	2517.36
Temperature (K)	293(2)	293(2)
Wavelength (Å)	0.71073	0.71073
Crystal system	trigonal	trigonal
Space group	R-3	R-3
a (Å)	17.976(2)	18.3083(7)
b (Å)	17.976(2)	18.3083(7)
c (Å)	27.338(3)	29.1307(8)
α (°)	90.00	90.00
β (°)	90.00	90.00
Γ (°)	120.00	120.00
Volume ($Å^3$), Z	7650.4(18), 6	8456.2(7), 6
F (000)	5796.0	6660.0
θ range for data collection(°)	3.01 to 29.54	3.47 to 26.73
Goodness-of-fit on F^2	1.045	1.044
Final R1[a], wR2[b]	0.0791, 0.1766	0.0517, 0.1252

[a]$R_1 = [|F_0| - |F_c|]/|F_0|$; [b]$wR_2 = [w(F_0^2 - F_c^2)^2]/[w(F_0^2)^2]^{1/2}$; $w = 1/[\sigma^2(F_o)^2 + 0.0297\ P^2 + 27.5680\ P]$, where $P = (F^2_o + 2\ F^2_c)/3$.

Table 4. Selected bond lengths and angles for complexes **1**–**4**.

Complex **1**			
Zn(1)–N(1)	2.011(3)	Zn(1)–N(3)	2.111(3)
Zn(1)–Cl(1)	2.2293(11)	Zn(1)–Cl(2)	2.1794(13)
N(3)–Zn(1)–N(1)	78.95(12)	N(3)–Zn(1)–Cl(1)	107.04(10)
N(3)–Zn(1)–Cl(2)	116.91(11)	N(1)–Zn(1)–Cl(1)	109.19(9)
N(1)–Zn(1)–Cl(2)	119.61(11)	Cl(1)–Zn(1)–Cl(2)	118.31(5)
Complex **2**			
Cd(1)–Cl(1)	2.678(3)	Cd(1)–Cl(1)#1	2.642(2)
Cd(1)–Cl(2)	2.546(3)	Cd(1)–Cl(2)#1	2.590(3)
Cd(1)–N(1)	2.443(10)	Cd(1)–N(2)	2.339(8)
Cl(1)–Cd(1)#1	2.642(2)	Cl(2)–Cd(1)#2	2.590(3)
Cl(1)–Cd(1)–Cl(2)	109.69(9)	Cl(1)–Cd(1)–Cl(1)#2	163.98(7)
Cl(2)#1–Cd(1)–Cl(1)	84.08(8)	Cl(2)–Cd(1)–Cl(2)#1	98.22(14)

New Journal of Chemistry Accepted Manuscript

N(1)–Cd(1)–Cl(1)	82.2(2)	N(2)–Cd(1)–N(1)	68.2(3)
N(2)–Cd(1)–Cl(1)	83.2(2)	N(2)–Cd(1)–Cl(1)#2	100.4(2)
N(2)–Cd(1)–Cl(2)#1	164.0(2)	N(2)–Cd(1)–Cl(2)	95.2(2)
Cl(2)–Cd(1)–Cl(1)#2	85.66(8)	N(1)–Cd(1)–Cl(1)#2	84.6(2)
Cl(2) #1–Cd(1)–Cl(1)#2	89.33(8)	N(1)–Cd(1)–Cl(2)	158.8(2)
N(1)–Cd(1)–Cl(2)#1	100.5(2)		
Complex **3**			
Hg(1)–Br(1)	2.529(2)	Hg(1)–Br(2)	2.465(2)
Hg(1)–N(2)	2.246(14)	Hg(1)–N(1)	2.437(16)
Hg(2)–Br(3)	2.409(4)	Hg(2)–Br(4)	2.419(4)
Hg(2)···Br(2)	3.229(23)	Hg(2)···Br(2)#1	3.227(33)
Hg(2)···Br(2)#2	3.229(24)	Br(2)–Hg(1)–Br(1)	124.57(7)
N(2)–Hg(1)–Br(1)	103.8(3)	N(2)–Hg(1)–Br(2)	125.7(4)
N(1)–Hg(1)–Br(1)	103.3(3)	N(1)–Hg(1)–Br(2)	115.4(3)
N(1)–Hg(1)–N(2)	69.3(5)	Br(4)–Hg(2)–Br(3)	180.0
Complex **4**			
Hg(1)–I(1)	2.6733(11)	Hg(1)–I(2)	2.6357(11)
Hg(1)–N(1)	2.320(9)	Hg(1)–N(3)	2.432(10)
Hg(2)–I(3)	2.6318(17)	Hg(2)–I(4)	2.6544(17)
Hg(2)···I(2)	3.3088(11)	Hg(2)···I(2)#1	3.3088(11)
Hg(2)···I(2)#2	3.3088(11)	I(2)–Hg(1)–I(1)	124.97(3)
N(1)–Hg(1)–I(1)	109.0(2)	N(1)–Hg(1)–I(2)	119.3(2)
N(1)–Hg(1)–N(3)	69.2(3)	N(3)–Hg(1)–I(1)	107.2(2)
N(3)–Hg(1)–I(2)	113.0(2)	I(4)–Hg(2)–I(3)	180.0

Symmetry transformations used to generate equivalent atoms: #1 1+Y-X,1-X,+Z; #2 1-Y,+X-Y,+Z for **1**. #1 2/3-Y+X,1/3+X,4/3-Z; #2 -1/3+Y,1/3-X+Y,4/3-Z; #3 2-Y,1+X-Y,+Z; #4 1+Y-X,2-X,+Z; #5 1+Y-X,1-X,+Z; #61-Y,+X-Y,+Z for **2**. #1 1+Y-X,1-X,+Z; #2 1-Y,+X-Y,+Z for **3**. #1 1-Y,+X-Y,+Z; #2 1+Y-X,1-X,+Z for **4.**

***In vitro* cytotoxicity assay.**

Complex **1** was dissolved in DMSO (cell culture reagent) just before the experiment, and a counted amount of complexes solution was added to the growth medium containing cells with a final solvent concentration of 5‰, which turns out to have no discernible effect on cell killing.

The growth inhibitory effect of the tittle complexes on human tumor cell lines was evaluated by means of MTT (MTT = 3-(4,5-dimethylthiazol-2-yl)-2,5-diphenyltetrazolium bromide) assay, in which MTT is cut down by living cells to produce a DMSO soluble (formazan) that could be detected through colorimetric analysis. Briefly, cells were seeded in 96-well microplates in growth medium (200 μL), and then incubated at 37°C in a highly humidified atmosphere with 5% CO_2. Amount of cells range from 4×10^3 to 8×10^3 cells/well, and the number relies on the growth characteristics of different cell lines to change. The medium was eliminated and replaced with a fresh one (200 μL) containing the complex at ten different concentrations (ranging from 10 μM to 50 μM) after 24 h. Three test timescale (24 h, 48 h, 72 h) were established for each treatment. After the special time, 20 μL of MTT solution (5 mg/mL) were added to each well and further incubation for 4 h at 37°C. Then the medium with MTT were discarded and 150 μL of DMSO was added to each well to dissolve the formazan crystals at room temperature. The absorbance was measured at test wavelength of 492 nm using a microplate reader. The % cell inhibition was determined as follow: % cell inhibition = (1-$Abs_{treated\ cells}/Abs_{control\ cells}$) × 100%. Results of complex **1** were expressed as IC_{50} values, which were determined by plotting the percentage viability versus concentration on a logarithmic graph and reading off the control. Each experiment was independently repeated three times, and the final IC_{50} values were calculated by the average of triplicate experimental results.

Acknowledgment

We gratefully acknowledge the financial support by the National Natural Science Foundation of China (Nos. 21371046 and 21401041), and the He'nan key science and technology research (Nos. 122102310061 and 132102310121), and the foundation of Training Program for young key teacher of Henan University of Urban Construction.

References

1 (a) K. J. Humphreys, K. D. Karlin and S. E. Rokita, *J. Am. Chem. Soc.,* 2002, **124**, 8055; (b) T. Kajiwara, N. Kon, S. Yokozawa, T. Ito, N. Iki and S. Miyano, *J. Am. Chem. Soc.,* 2002, **124**, 11274; (c) X. X. Zhou, H. C. Fang, Y. Y. Ge, Z. Y. Zhou, Z. G. Gu, X. Gong, G. Zhao, Q. G. Zhan, R. H. Zeng and Y. P. Cai, *Cryst. Growth Des.,* 2010, **10**, 4014; (d) I. A. Riddell, Y. R. Hristova, J. K. Clegg, C. S. Wood, B. Breiner and J. R. Nitschke, *J. Am. Chem. Soc.,* 2013, **135**, 2723; (e) C. D. Zhang, S. X. Liu, C. Y. Sun, F. J. Ma and Z. M. Su, *Cryst. Growth Des.,* 2009, **9**, 3655.

2 (a) D. Sun, G. G. Luo, N. Zhang, R. B. Huang and L. S. Zheng, *Chem. Commun.,* 2011, **47**, 1461; (b) D. Sun, L. L. Zhang, H. F. Lu, S. Y. Feng and D. F. Sun, *Dalton Trans.,* 2013, **42**, 3528; (c) D. Sun, D. F. Wang, X. G. Han, N. Zhang, R. B. Huang and L. S. Zheng, *Chem. Commun.,* 2011, **47**, 746; (d) D. Sun, H. Wang, H. F. Lu, S. Y. Feng, Z. W. Zhang, G. X. Sun and D. F. Sun, *Dalton Trans.,* 2013, **42**, 6281; (e) D. Sun, F. J. Liu, R. B. Huang and L. S. Zheng, *Inorg. Chem.,* 2011, **50**, 12393.

3 W. T. Chen, M. S. Wang, X. Liu, G. C. Guo and J. S. Huang, *Cryst. Growth Des.,* 2006, **6**, 2289.

4 (a) C. Orvig, D. J. Berg and S. J. Rettig, *J. Am. Chem. Soc.,* 1991, **113**, 2528; (b) R. M. Kirchner, C. Mealli, M. Bailey, M. Howe, L. P. Torre, L. J. Wilson, L. C. Andrews, N. J. Rose and E. C. Lingafelter, *Coord. Chem. Rev.,* 1987, **77**, 89; (c) K. G. Raghunathan and P. K. Bharadwaj, *J. Chem. Soc., Dalton Trans.,* 1992, 2417; (d) P. Ghosh, R. Shukla, D. K. Chand and P. K. Bharadwaj, *Tetrahedron.,* 1995, **51**, 3265; (e) T. N. Sorrell, W. E. Allen and P. S. White, *Inorg. Chem.,* 1995, **34**, 952; (f) A. Mohamadou and C. Gerard, *J. Chem. Soc., Dalton Trans.,* 2001, 3320.

5 (a) W. Y. Sun, J. Fan, T. Okamura, J. Xie, K. B. Yu and N. Ueyama, *Chem. Eur. J.,* 2001, **7**, 2557; (b) J. Fan, H. F. Zhu, T. Okamura, W. Y. Sun, W. X. Tang and N. Ueyama, *Chem. Eur. J.,* 2003, **9**, 4724; (c) J. Fan, H. F. Zhu, T. Okamura, W. Y. Sun, W. X. Tang and N. Ueyama, *Inorg. Chem.,* 2003, **42**, 158; d) H. K. Liu, W. Y. Sun, W. X. Tang, T. Yamamoto and N. Ueyama, *Inorg. Chem.,* 1999, **38**, 6313.

New Journal of Chemistry Accepted Manuscript

6 X. Q. Yao, D. P. Cao, J. S. Hu, Y. Z. Li, Z. J. Guo and H. G. Zheng, *Cryst. Growth Des.,* 2011, **11**, 231.

7 (a) W. L. Jia, T. McCormick, Y. Tao, J. P. Lu and S. N. Wang, *Inorg. Chem.,* 2005, **44**, 5706; (b) Q. D. Liu, W. L. Jia and S. N. Wang, *Inorg. Chem.,* 2005, **44**, 1332.

8 S. Y. Wan, Y. Z. Li, Taka-aki. Okamura, J. Fan, W. Y. Sun and N. Ueyama, *Eur. J. Inorg. Chem.,* 2003, 3783.

9 (a) X. P. Yang, B. S. Kang, W. K. Wong, C. Y. Su and H. Q. Liu, *Inorg. Chem.,* 2003, **42**, 169; (b) Z. R. Pan, H. G, Zheng, T. Wang, Y. Song and Y. Li, *Inorg. Chem.,* 2008, **47**, 9528.

10 M. Prabhakar, P. S. Zacharias and S. K. Das, *Inorg. Chem.,* 2005, **44**, 2585.

11 M. Dakanali, E. T. Kefalas, C. P. Raptopoulou, A. Terzis, T. Mavromoustakos and A. Salifoglou, *Inorg. Chem.,* 2003, **42**, 2531.

12 E. Freire, S. Baggio, R. Baggio and L. Suescun, *J. Chem. Cryst.,* 1999, **29**, 825.

13 (a) W. T. Chen, M. S. Wang, X. Liu, G. C. Guo and J. S. Huang, *Cryst. Growth Des.,* 2006, **6**, 2289; (b) L. R. Falvello, J. Fornies, A. Martin, R. Navarro, V. Sicilia and P. Villarroya, *Inorg. Chem.,* 1997, **36**, 6166; (c) X. J. Zhang, W. T. Yu, Y. Xie, Q. R. Zhao and Y. P. Tian, *Inorg. Chem. Commun.,* 2003, **6**, 1338.

14 (a) A. Bondi, *J. Phys. Chem.,* 1964, **68**, 441; (b) A. Bondi, *J. Phys. Chem.,* 1966, **70**, 3006; (c) A. Gavezzotti, *J. Am. Chem. Soc.,* 1983, **105**, 5220.

15 (a) Y. B. Dong, P. Wang, R. Q. Huang and M. D. Smith, *Inorg. Chem.,* 2004, **43**, 4727; (b) G. Wu, X. F. Wang, T. Okamura, W. Y. Sun and N. Ueyama, *Inorg. Chem.,* 2006, **45**, 8523.

16 (a) S. Yuan, Y. K. Deng and D. Sun, *Chem. Eur. J.,* 2014, **20**, 10093; (b) B. X, J. Xie, H. M. Hu, X. L. Yang, F. X. Dong, M. L. Yang and G. L. Xue, *Cryst. Growth Des.,* 2014, **14**, 1629; (c) D. Sun, Z. H. Yan, V. A. Blatov, L. Wang and D. F. Sun, *Cryst. Growth Des.*, 2013, **13**, 1277.

17 S. N. Zhao, S. Q. Su, X. Z. Song, M. Zhu, Z. M. Hao, X. Meng, S. Y. Song and H. J. Zhang, *Cryst. Growth Des.,* 2013, **13**, 2756.

18 (a) C. M. Che, C. W. Wan, W. Z. Lin, W. Y. Yu, Z. Y. Zhou, W. Y. Lai and S. T. Lee, *Chem. Commun. (Cambridge, U.K.),* 2001, 721; (b) T. L. Hu, R. Q. Zou, J. R. Li and X. H. Bu, *J. Chem. Soc., Dalton Trans.* 2008, 1302; (c) Q. G. Zhai, X. Y. Wu, S. M. Chen, C. Z. Lu and W. B. Yang, *Cryst. Growth Des*., 2006, **6**, 2126; (d) S. L. Zheng, J. H. Yang, X. L. Yu, X. M. Chen and W. T. Wong, *Inorg. Chem.,* 2004, **43**, 830.

19 (a) K. M. C. Wong, L. L. Hong, W. H. Lam, N. Zhu and V. W. W. Yam. *J. Am. Chem. Soc.,* 2007, **129**, 4350; (b) H. Y. Chao, W. Lu, Y. Li, M. C. W. Chan, C. M. Che, K. K. Cheung and N. Zhu, *J. Am. Chem. Soc.,* 2002, **124**, 14696.

20 D. Sun, L. L. Zhang, H. F. Lu, S. Y. Feng and D. F. Sun, *Dalton Trans.,* 2013, **42**, 3528.

21 M. A. Omary and H. H. Patterson, *Inorg. Chem*., 1998, **37**, 1060.

22 H. W. Liu, F. Zhao, R. Y. Yang, M. Y. Wang, M. Q. Zheng, Y. S. Zhao, X. Zhang, F. Qiu and H. S. Wang, *Phytochemistry*., 2009, **70**, 773.

23 (a) D. Pucci, A. Crispini, B. S. Mendiguchía, S. Pirillo, M. Ghedini, S. Morelli and L. D. Bartolo, *Dalton Trans.,* 2013, **42**, 9679; (b) J. Zhao, S. S. Li, D. D. Zhao, S. F. Chen, J. Y. Hu, *J. Coord. Chem.,* 2013, **66**, 1650.

24 (a) N. L. J. Vekshin, *Biol. Phys.,* 1999, **25**, 339; (b) Y. B. Yin, Y. N. Wang and J. B. Ma, *Spectrochim Acta A.,* 2006, **64**, 1032; (c) D. A. Yushchenko, O. B. Vadzyuk, S. O. Kosterin, G. Duportail, Y. Mély and V. G. Pivovarenko, *Anal. Biochem.,* 2007, **369**, 218.

25 R. W. Y. Sun, K. L. Li, D. L. Ma, J. J. Yan, C. N. Lok, C. H. Leung, N. Zhu and C. M. Che, *Chem. Eur. J.,* 2010, **16**, 3097.

26 B. B. Schaack, W. Schrader and F. Schüth, *J. Phys. Chem. B*, 2009, **113**, 11240.

27 (a) A. W. Addison and P. J. Burke, *J. Heterocycl. Chem*., 1981, **18**, 803; (b) A. Yoshimura, K. Nozaki, N. Ikeda and T. Ohno, *Bull. Chem. Soc. Jpn.,* 1996, **69**, 2791.

28 (a) G. M. Sheldrick, SHELXTL-97, *Program for Crystal Structure Refinement,* University of Göttingen, Germany, 1997; (b) G. M. Sheldrick, SHELXS-97, *Program for Crystal Structure Solution,* University of Göttingen, Germany, 1997; (c) G. M. Sheldrick, *Acta Crystallogr. Sect.* 2008, **A64**, 112; (d) O. V. Dolomanov, L. J. Bourhis, R. J. Gildea, J. A. K. Howard and H. Puschmann, *J. Appl. Cryst.,* 2009, **42**, 339.

29 (a) P. Van der Sluis and A. L. Spek, *Acta Crystallogr., Sect. A*, 1990, **46**, 194; (b) A. L. Spek, *J. Appl. Crystallogr.*, 2003, **36**, 7.

New Journal of Chemistry Accepted Manuscript